Supplemental Information

Disentangling the Complex Vibrational Mechanics of the Protonated Water Trimer by Rational Control of Its Hydrogen Bonds

Chinh H. Duong[a], Nan Yang[a], and Mark A. Johnson[a,*]
[a]Sterling Chemistry Laboratory, Yale University, New Haven, Connecticut 06520, USA

Ryan J. DiRisio,[b] Anne B. McCoy[b,*]
[b]Department of Chemistry, University of Washington, Seattle, Washington 98195, USA

Qi Yu,[c] Joel M. Bowman[c,*]
[c]Department of Chemistry and Cherry L. Emerson Center for Computational Science, Emory University, Atlanta, Georgia 30322, USA

*Corresponding Authors:
M. A. Johnson. Tel: +1 203 432 5226, Email: mark.johnson@yale.edu
A. B. McCoy. Tel: +1 206 543 7464, Email: abmccoy@uw.edu
J. M. Bowman. Tel: +1 404 727 6592, Email: jmbowma@emory.edu

Contents:

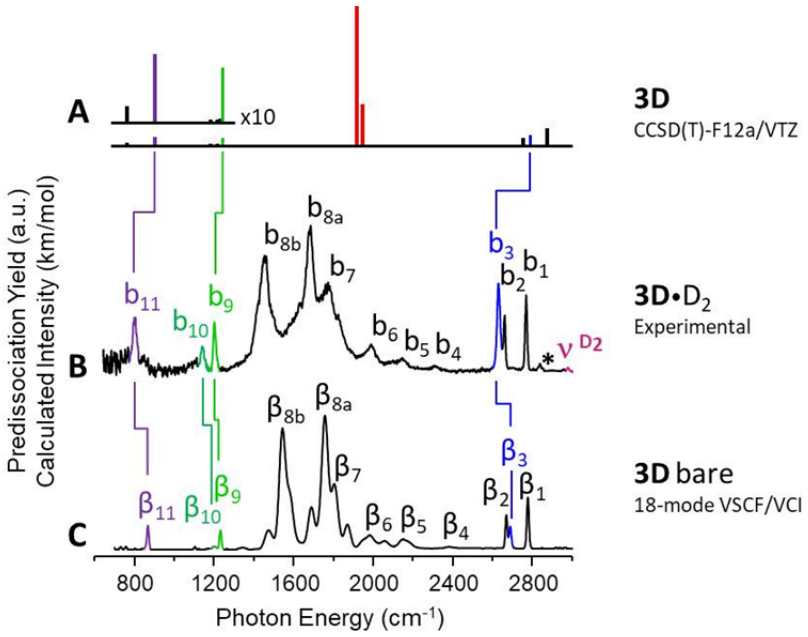

Figure S1. Comparison of the (A) CCSD(T)-F12a/VTZ harmonic spectrum, (B) D_2-tagged vibrational predissociation spectrum, and (C) 18-mode VSCF/VCI calculated spectrum of **3D**. Traces A-C are reproduced from ref. 1 with permission from the American Chemical Society.

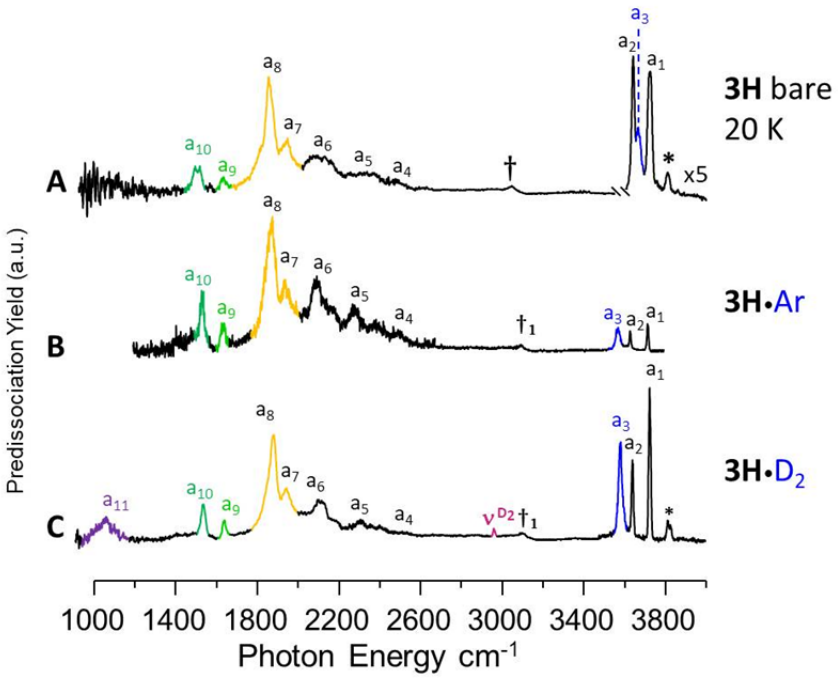

Figure S2. Comparison of the predissociation spectra of (A) **3H** bare with (B) **3H**·Ar and (C) **3H**·D_2 tags. Traces A and C are adapted from ref. 1 with permission from the American Chemical Society.

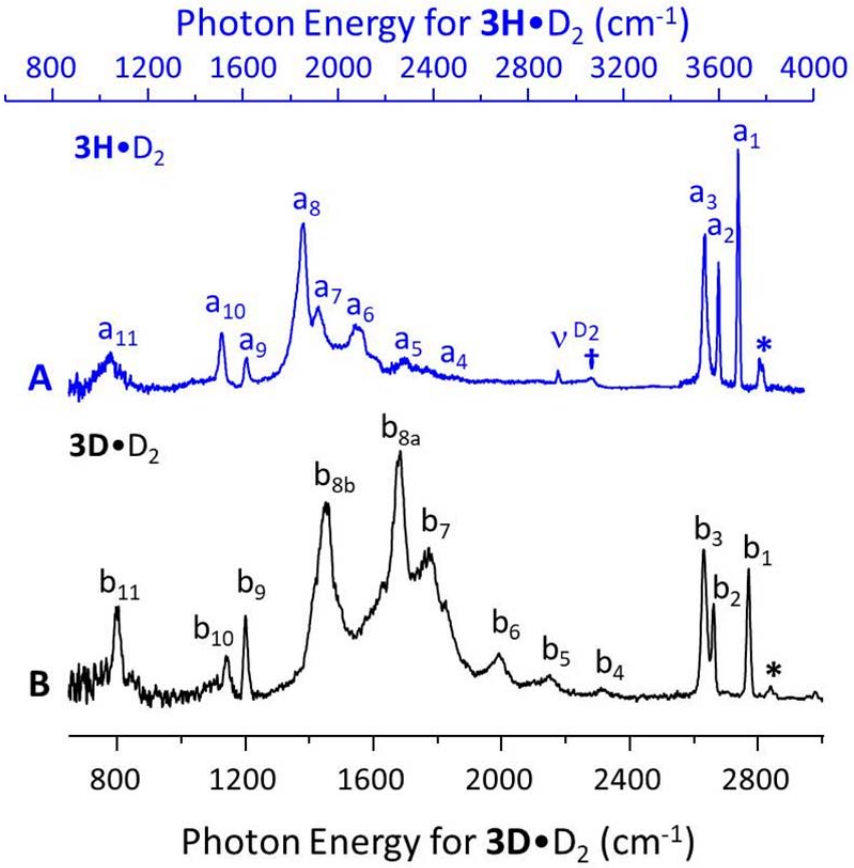

Figure S3. Vibrational predissociation spectrum of (A) **3H**·D_2 (blue trace/top scale) with the wavenumbers scaled by 1/1.36 compared with that of (B) **3D**·D_2 (black trace/bottom scale). Trace A and B were adapted from ref. 1 with permission from the American Chemical Society.

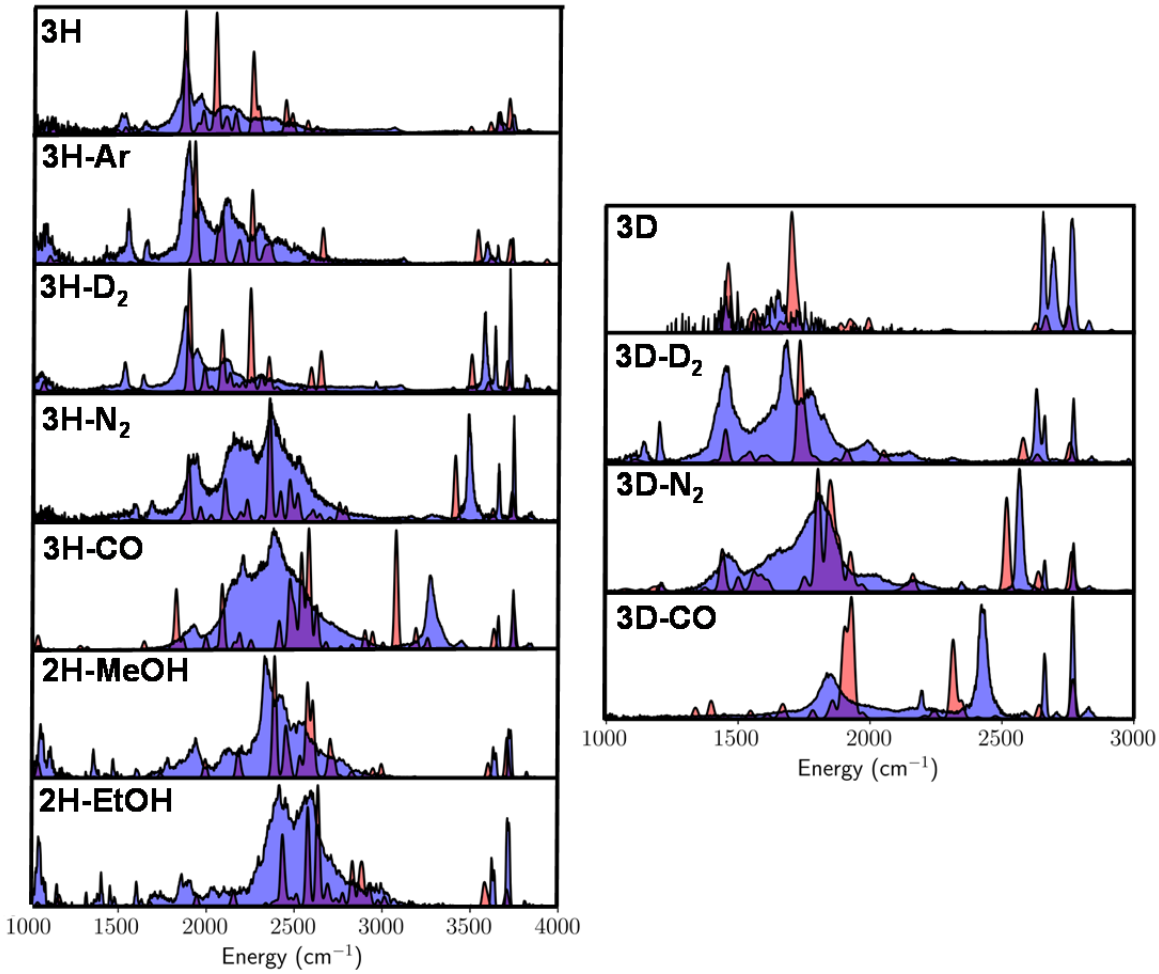

Figure S4. Comparison of experimental spectra for **3H**·X, **3D**·X, **2H**·MeOH·H_2, and **2H**·EtOH·H_2 (blue) to the aug-cc-pVDZ anharmonic (VPT2) spectra (red) of **3H**·X, **3D**·X, **2H**·MeOH, and **2H**·EtOH, where X=Ar, D_2, N_2, CO. The baseline of the spectra has been shifted and both spectra have been scaled to have equal values for the largest signal. Regions where the two spectra overlap are shown in purple.

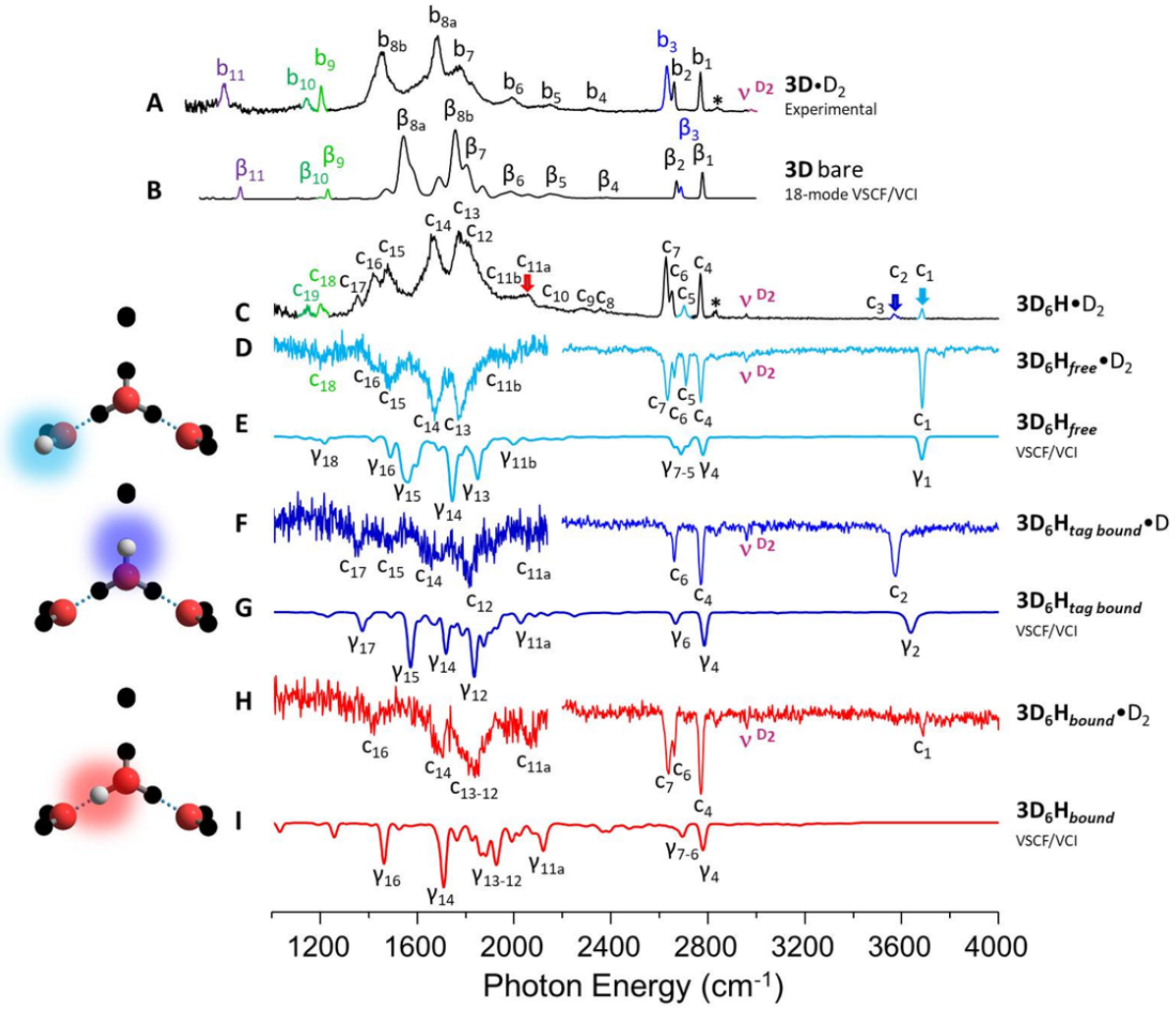

Figure S5. Comparison of the (A) predissociation spectrum of **3D** with D_2 messenger tag, (B) **3D** bare 18-mode VSCF/VCI calculated spectrum, and (C) predissociation spectrum of $\mathbf{HD_6O_3^+}\cdot D_2$. The isotopomer-selective spectra of $HD_6O_3^+\cdot D_2$ ($\mathbf{3D_6H}\cdot D_2$) is shown as depletion spectra (inverted traces) corresponding to the positions of the H atom at (D) the free OH of a flanking water ($\mathbf{3D_6H}_{free}$), (F) the tag bound free OH of the hydronium core ($\mathbf{3D_6H}_{tag\ bound}$), and (H) the shared proton position of the hydronium core and an exterior water ($\mathbf{3D_6H}_{bound}$) with the corresponding VSCF/VCI calculations (E), (G), and (I) shown underneath each experimental trace, respectively. The colored arrows indicate the probe positions of the laser at 3685 cm^{-1} (light blue), 3572 cm^{-1} (dark blue), and 2049 cm^{-1} (red). Trace (H) also includes spectral contributions from the $\mathbf{3D_6H}_{free}$ isotopologue because the probe position at 2049 cm^{-1} overlaps with some spectral signature of the $\mathbf{3D_6H}_{free}$, but dominantly has features of the $\mathbf{3D_6H}_{bound}$. Traces A and B were adapted from ref. 1 with permission from the American Chemical Society.

Table S1. Cartesian coordinates for the optimized geometries for the complexes described in the text. All optimizations, unless otherwise specified, were performed at the MP2/aug-cc-pVDZ level of theory and basis, using very tight convergence. The Cartesian coordinates for **3H** at the CCSD(T)-F12a/VTZ level of theory is also included.

3H (CCSD(T)-F12a/VTZ)

H	1.7491200611	-0.0796214950	0.0000000000
H	0.3439059486	-0.2140113235	0.8689463747
H	0.3439059486	-0.2140113235	-0.8689463747
O	0.8513606628	-0.4310220136	0.0000000000
H	-0.5625577669	0.8116970646	2.5631675028
H	-0.6119572769	-0.7283452143	2.7127202516
O	-0.4345874853	-0.0158831079	2.0923462443
H	-0.5625577669	0.8116970646	-2.5631675028
H	-0.6119572769	-0.7283452143	-2.7127202516
O	-0.4345874853	-0.0158831079	-2.0923462443

3H

O	2.0806000347	-0.4759731840	-0.0042579152
H	2.5692803500	-0.7766810743	0.7753016082
H	2.7184227788	-0.4288690485	-0.7315134676
O	0.0012598151	0.9136380260	-0.0726813536
H	0.0035383837	1.6875908628	0.5133258638
H	-0.8734694963	0.3624632875	0.0152096195
H	0.8730436807	0.3577309948	0.0146687762
O	-2.0855372061	-0.4646849837	-0.0029676488
H	-2.7235513586	-0.4141174079	-0.7298226373
H	-2.5753499817	-0.7627524727	0.7768951545

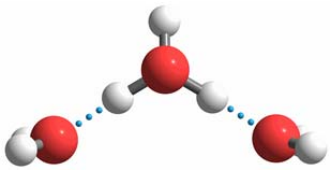

3H·Ar

H	-0.0011522191	0.0481666694	-0.0016031659
O	0.0059462683	0.1680587026	0.9587244008
H	0.9291252741	0.0912087367	1.2406092373
O	-1.8483131098	-0.2909242061	2.5865591428
H	-2.3114710328	-1.1375646014	2.4560272246
H	-2.5077473667	0.4980716834	2.6902188718
H	-1.1142684601	-0.1385740167	1.8751652647
O	-3.3427882241	1.6980122273	2.9174150595
H	-3.4428026597	2.0886416444	3.7977730929
H	-4.1357548998	1.9371563854	2.4167479936
Ar	-3.3711011292	-3.2614213155	2.3033640410

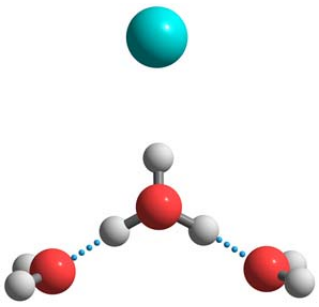

3H·D_2

O	2.086861868	-0.668632595	0.090966138
H	2.575869197	-0.760656052	0.920973567
H	2.720293737	-0.831173958	-0.623053591
O	0.000342903	0.661076141	-0.346043561
H	0.866342421	0.149429778	-0.115542632
H	-0.866250222	0.149943122	-0.116636848
H	0.000387211	1.569720899	0.010020275
O	-2.087512118	-0.667398387	0.088330913
H	-2.720131106	-0.829574685	-0.626492048
H	-2.577630788	-0.759116690	0.917716407
H(Iso=2)	0.000365682	3.259927215	0.851992278
H(Iso=2)	0.000861206	3.447124212	0.117258103

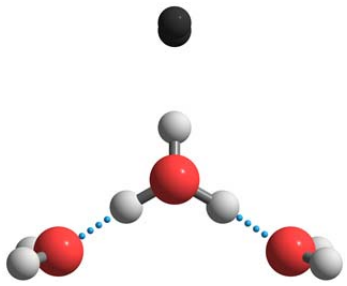

3H·N_2

H	-0.0000480764	0.0005011582	0.0000258235
O	-0.0002002547	-0.0001242434	0.9675313421
H	0.9275096034	-0.0000747760	1.2439569632
O	-1.8063335934	-0.7826024716	2.5439876673
H	-2.1923994438	-1.6597947607	2.3382282413
H	-2.5258916662	-0.0694087749	2.7141330988
H	-1.0977155555	-0.4969700664	1.8572322951
O	-3.4738945869	1.0397845014	3.0516861088
H	-3.5973001721	1.3545139885	3.9587544399
H	-4.2745813128	1.2801522209	2.5646631974
N	-2.8866324427	-3.4480810859	2.0733214065
N	-3.2698284991	-4.5057506899	1.9623174161

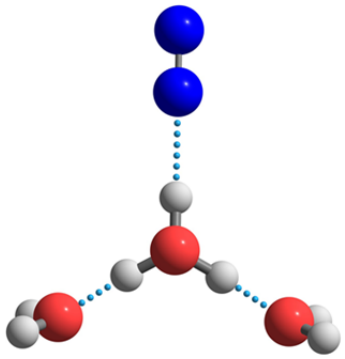

3H·CO

H	-3.4014017100	-4.8679916000	1.8855265400
O	-3.3777697000	-3.9685986900	0.2944653010
H	-3.9380549700	-5.1526537000	-0.9816949790
O	-0.9875025650	-0.0000021781	-0.9147559880
H	0.8374438790	-0.0000057008	-0.5010151270
H	-1.8797850200	1.6131760400	-0.3370167820
H	-1.8797914300	-1.6131755500	-0.3370150300
O	-3.3777600500	3.9686050000	0.2944646910
H	-3.9380495300	5.1526569000	-0.9816983270
H	-3.4013752100	4.8680111800	1.8855211400
C	4.4537154300	-0.0000076074	0.0076883571
O	6.6028724900	-0.0000006170	0.2409837990

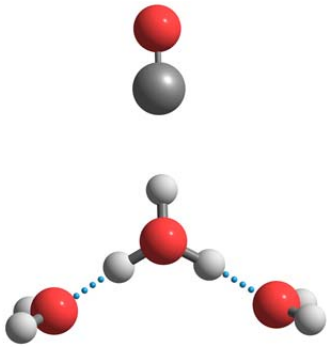

2H·MeOH

H	0.0000016132	0.0000021993	-0.0000001821
O	0.0000000102	0.0000013246	0.9677192141
H	0.9299802072	0.0000001535	1.2372218405
O	-1.7951230747	0.7877072412	2.5851129518
C	-2.7492384077	-0.3176112395	2.8305098039
H	-2.2696797764	1.6680037931	2.3905468190
H	-1.0979965991	0.5439776557	1.8832635992
O	-3.0848406598	2.9593710050	2.3033064807
H	-2.9265844943	3.6997014360	2.9069294642
H	-3.4823950566	3.3407603190	1.5077101261
H	-2.1443801268	-1.1821491692	3.1190826961
H	-3.3301444443	-0.5129980650	1.9217070680
H	-3.3867409850	0.0096790693	3.6569631881

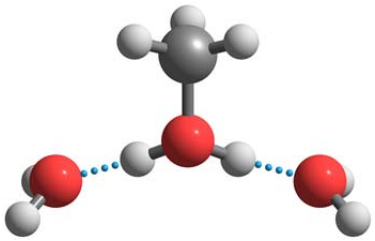

2H·EtOH

H	-2.0297270700	5.1915563800	1.4908967600
O	-2.2263653400	3.9482204800	0.1637973160
H	-2.9574309600	4.8448804600	-1.2542580500
O	0.4224211180	-0.0267913009	-0.6499859230
C	-0.7057868720	-2.2427042000	0.7108756170
H	2.3059924700	0.1318098470	-0.3166136890
H	-0.5176359370	1.6049667300	-0.2757993330
O	5.2044405600	-0.0403410393	0.0095973699
H	6.3328555700	-0.1097394480	-1.4285829600
H	6.2003669800	0.5952501310	1.4050553000
C	-3.3597287800	-2.6475505200	-0.2677941890
H	-0.6360234730	-1.8250137800	2.7429385000
H	0.5746834920	-3.8069651800	0.2567458110
H	-3.3488582500	-3.0141215800	-2.3112558200
H	-4.5742028300	-1.0137423900	0.1475463160
H	-4.1608967900	-4.3060579400	0.6975684900

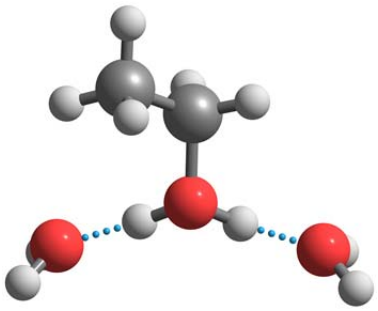

Table S2. Table of proton affinities gathered from NIST.[2]

Molecule or Atom	Proton Affinities (kJ/mol)
He	177.8
Ar	369.2
H_2	422.3
N_2	493.8
CO	594
H_2O	691

Table S3. Band labels, experimental frequencies and assignments for **3H**·X where X=Ar, D_2, N_2, CO, and H_2O. Assignments from VSCF/VCI are based on ref. 1 with complicated mixed state bands involving the IHB simplified to "Mixed states involving the IHB".

Label 3H·Ar	**Exp.[a] 3H·Ar**	**Label 3H·D_2**	**Exp.[a] 3H·D_2**	**Label 3H·N_2**	**[a]Exp.[a] 3H·N_2**	**Label 3H·CO**	**Exp.[a] 3H·CO**	**Label 4H·D_2**	**Exp.[a] 4H·D_2**	**VSCF/VCI assignments for 3H[b] and 4H·D_2[c]**
*	-	*	3814, 3828	*	3827	*	3814, 3830	*	3815, 3850	H_2O antisym. stretch + H_3O^+ torsion[3]
a_1	3722	a_1	3726	n_1	3725	co_1	3728	a_1	3733	Free OH antisym. H_2O stretch
								a_2	3724	Free OH antisym. AD H_2O stretch
a_2	3635	a_2	3640	n_2	3640	co_2	3644	a_3	3648	Free OH sym. H_2O stretch
								a_4	3636	Free OH sym. AD H_2O stretch
a_3	3577	a_3	3580	n_3	3468	co_3	3259			Free OH H_3O^+ stretch
ǂ$_1$	3100	**ǂ$_1$**	3102							Complicated comb. band + IHB antisym. stretch
				ǂ$_1$	3261[d]	**ǂ$_1$**	3433[d]			
				ǂ$_2$	3145[d]	**ǂ$_2$**	2879[d]			
a_4	2501	a_4	2520	n_4	2502	co_4	2517			Mixed states involving the IHB
		ν^{D_2}	2961	ν^{N_2}	-	ν^{CO}	-	-	-	D_2/N_2/CO stretch[e]
								$a_{5\text{-}7}$	2653	Complex combination bands involving H_3O^+ ν_{as} + rotation + bend
a_5	2283	a_5	2307	n_5	2344	co_5	2374			Mixed states involving the IHB
								a_8	2300	H_3O^+ rotation + H_2O bend
								a_9	2237	H_3O^+ rotation + bend
a_6	2097	a_6	2109	n_6	2173	co_6	2191			Mixed states involving the IHB
a_7	1945	a_7	1943	n_7	1923	co_7	1909			Mixed states involving the IHB
a_8	1874	a_8	1878	n_8	1896			a_{10}	1904	Mixed states involving the IHB
a_9	1640	a_9	1639	n_9	1666					H_3O^+ bend
a_{10}	1537	a_{10}	1534	n_{10}	1573					H_2O bend + IHB antisym. stretch
								a_{11}	1766	H_3O^+ umbrella + D_3O^+ rotation about the A and B axes
								a_{12}	1616	H_3O^+ and HOH bends
a_{11}	1060	a_{11}	1059	n_{11}	1068					H_3O^+ umbrella
↓	2099	↓	2100	↓	2250	↓	2344	↓	2649	Calculated Centroid[f]

[a]Experimental frequencies are accurate within ±4 cm^{-1}.
[b]Assignments are based on VSCF/VCI calculations reported in ref. 1 and details on the "Mixed states involving the IHB" can be found there.
[c]Assignments are based on VPT2 calculations reported in ref. 4.
[d]Unassigned features.
[e]Assigned based on proximity to D_2 stretch fundamental at 2993.6 cm^{-1} and not VSCF/VCI calculations.[5]
[f]Centroid calculated as $\sum_j \omega_j I_j / \sum_j I_j$, the average intensity (I) weighted frequency (ω) within a select spectral region specified in the captions of Figure 3 and 4.

Table S4. Band labels and experimental frequencies for **2H**·MeOH·H_2 and **2H**·EtOH·H_2 with the VPT2 assignments of **2H**·MeOH and **2H**·EtOH.

Label 2H·MeOH·H_2	**Exp.[a] 2H·MeOH·H_2**	**VPT2[b,c] 2H·MeOH**	**Label 2H·EtOH·H_2**	**Exp.[a] 2H·EtOH·H_2**	**VPT2[b,c] 2H·EtOH**	**VPT2 Assignments[c]**
*	3816	3758-3823[c]	*	3811	3760-3814[d]	Outer H_2O antisym. OH stretch + outer H_2O rotation[3]
Me_1	3725	3704	Et_1	3721	3709	Outer H_2O antisym. OH stretch
Me_2	3714	3704	Et_2	3712	3698	Outer AD H_2O antisym. OH stretch
Me_3	3640	3598	Et_3	3637	3601	Outer H_2O sym. OH stretch
Me_4	3627	3597	Et_4	3622	3592	Outer AD H_2O sym. OH stretch
‡₁	3003	2943, 2989	**‡₁**	2968	2834-2927[d]	ROH_2^+ HOH bend + ROH_2^+ HOH rock
‡₂	2760	2699-2724[d]	**‡₂**	-----		ROH_2^+ HOH bend + ROH_2^+ umbrella or wag; ROH_2 HOH rock overtone
Me_5	2535	2571	Et_5	2579	2635	In-phase ROH_2^+ IHB
Me_6	2417	2370-2531[d]			2449, 2513	ROH_2^+ IHB + low-frequency modes; ROH_2^+ HOH rock + ROH_2^+ umbrella
Me_7	2340	2385	Et_6	2413	2578	Out-of-phase ROH_2^+ IHB
Me_8	2197				2432, 2438	ROH_2^+ HOH bend + RHO_2^+ HOH rotation
Me_9	2115	1733-2189[d]	Et_7	2040	1944-2160[d]	Overtones and combination
Me_{10}	1935		Et_8	1883	1679	bands involving ROH_2^+ HOH
Me_{11}	1771		Et_9	1709		rotations and umbrella
Me_{12}	1599	1556, 1579	Et_{10}	1603	1549, 1584	Outer H_2O bend
Me_{13}	1465	1449	Et_{11}	1453	1438, 1468	CH_3 bends
			Et_{12}	1403	1363, 1396	CH bends
Me_{14}	1353	1357				ROH_2^+ HOH rock
			Et_{13}	1319	1304	ROH_2^+ HOH rock
Me_{15}	1105	1140, 1152	Et_{14}	1149	1161, 1165	ROH_2^+ umbrella or HOH rotation or CO stretch + low-frequency modes
Me_{16}	1055	1038	Et_{15}	1047	1041	ROH_2^+ umbrella
↓	2312		↓	2451		Calculated Centroid[e]

[a]Experimental frequencies are accurate within ±4 cm^{-1}.

[b]Based on VPT2 calculations evaluated at the MP2/aug-cc-pVDZ level of theory and basis. When a range is provided there are multiple transitions to states with similar character in this frequency range.

[c]VPT2 frequencies are listed in increasing cm^{-1}, and the listed assignments are based on this calculation. Where several calculated transitions lie close to a feature in the spectrum, the specific assignment is not conclusive.

[d]Frequency ranges are reported for the VPT2 results when three or more transitions contribute intensity in the reported frequency range.

[e]Centroid calculated as $\sum_j \omega_j I_j / \sum_j I_j$, the average intensity (I) weighted frequency (ω) within a select spectral region specified in the captions of Figure 3 and 4.

Table S5. Band labels, experimental frequencies and assignments for 3**D**·X where X=D_2, N_2, CO, and D_2O. Assignments which were complex from ref. 1 and 4 were simplified with "Mixed states involving the IDB" or "Mixed states involving D_3O^+/DOD bends".

Label 3D·D_2	**Exp.[a] 3D·D_2**	**Exp.[a] 3D·N_2**	**Exp.[a] 3D·CO**	**Label 4D·D_2**	**Exp.[a] 4D·D_2**	**VSCF/VCI assignments for 3D[b] and 4D·D_2[c]**
*	2840	2828	2827	*	2822	D_2O antisym. stretch + D_3O^+ torsion[3]
b_1	2770	2767	2768	b_1	2772	Free OD antisym. D_2O stretch
				b_2	2765	Free OD antisym. AD D_2O stretch
b_2	2631	2658	2661	b_3	2664	Free OD sym. D_2O stretch
				b_4	2657	Free OD sym. AD D_2O stretch
b_3	2660	2564	2429			Free OD D_3O^+ stretch
b_4	2314	2424	-			Combination band of D_3O^+ bend + D_2O bend
$\nu^{D_2/N_2/CO}$	2978	2344	2195	ν^{D_2}	-	D_2/N_2/CO stretch[d]
				$\dagger_1$	2348	Mixed states involving the IDB
b_5	2149	2164	-			Mixed states involving the IDB
				$b_{5\text{-}6}$	2048	Mixed states involving the IDB
b_6	1991	2010	-			Low freq. modes + D_3O^+ rotation + wag + umbrella
b_7	1770	1799	1847	b_7	1999	IDB OD stretch
b_{8a}	1680	1651	1688			Mixed states involving the IDB
				b_8	1686	Mixed states involving D_3O^+/DOD bends
b_{8b}	1452	1459				Mixed states involving the IDB
b_9	1202	1206				D_3O^+ bend
				b_9	1639	D_3O^+/DOD bends + frustrated rotation of D_3O^+
b_{10}	1143					D_2O bend
				b_{10}	1402, 1459	D_3O^+ umbrella + D_3O^+ rotation about A and B axes
				b_{11}	1301	
b_{11}	800					D_3O^+ umbrella
				b_{12}	1198	D_3O^+ and DOD bends
↓	1664	1744	1866	↓	2024	Calculated Centroid

[a]Experimental frequencies are accurate within ±4 cm^{-1}.
[b]Assignments are based on VSCF/VCI calculations reported in ref. 1.
[c]Assignments are based on VPT2 calculations reported in ref. 4.
[d]Assigned based on proximity to D_2 stretch fundamental[5] at 2993.6 cm^{-1}, the CO stretch frequency[6] at 2148 cm^{-1} and the N_2 stretch frequency[7] at 2358.57 cm^{-1} and not VSCF/VCI calculations.

Table S6. Frequencies (harmonic (ω), anharmonic (ν) and deperturbed anharmonic (depert) and intensities of intense features in the calculated spectra between 1000 and 3000 cm^{-1} for **3H** and below 2200 cm^{-1} for **3D** of the systems for which spectra are reported in Figures 3 and 4, evaluated at the MP2/aug-cc-pVDZ level of theory and basis as implemented in Gaussian 16 (G16.A03).[8] A complete list of the calculated frequencies and intensities is provided in an EXCEL workbook.

3H

Vibration	ω (harm) (cm^{-1})	ν (anharm) (cm^{-1})	I (harm) (km mol^{-1})	I (anharm) (km mol^{-1})	Depert (cm^{-1})
in-phase IHB	2630.15	2279.18	1146.44	259.95	2174.26
out-of-phase IHB	2496.62	1863.14	3972.96	1223.29	2023.84
out-of-phase H_2O bend/H_3O^+ wag	1687.27	1628.38	62.82	5.75	1612.94
in-phase H_2O bend/H_3O^+ HOH bend	1683.02	1545.60	13.49	3.48	1541.81
in-phase H_2O bend/H_3O^+ HOH bend	1621.37	1606.66	3.72	1.21	1541.81
out-of-phase H_2O bend/H_3O^+ wag	1591.08	1519.41	1.98	59.93	1589.18
IHB out-of-plane bend (H_3O^+ umbrella)	1248.56	1101.33	213.57	159.55	1099.46
H_3O^+ rotation about symmetry axis	1072.70	1012.53	71.67	43.40	1009.77
overtone - out-of-plane bend	2497.12	2040.24		164.33	2130.91
overtone - H_3O^+ rotation	2145.40	1933.92		86.83	1933.91*
combination – out-of-plane bend + H_3O^+ rotation	2321.26	2247.13		819.66	2086.43

3H·Ar

Vibration	ω (harm) (cm^{-1})	ν (anharm) (cm^{-1})	I (harm) (km mol^{-1})	I (anharm) (km mol^{-1})	Depert (cm^{-1})
in-phase IHB	2685.99	2341.87	1274.69	268.02	2341.87
out-of-phase IHB	2566.95	2239.52	3713.51	947.37	2239.52
out-of-phase H_2O bend/H_3O^+ wag	1688.46	1621.98	65.19	15.66	1621.98
in-phase H_2O bend/H_3O^+ HOH bend	1685.20	1558.82	10.39	4.61	1558.82
in-phase H_2O bend/H_3O^+ HOH bend	1622.86	1627.22	2.41	1.54	1627.22
out-of-phase H_2O bend/H_3O^+ wag	1598.68	1542.39	6.69	15.70	1542.39
IHB out-of-plane bend (H_3O^+ umbrella)	1239.02	1089.27	205.92	101.51	1089.27
H_3O^+ rotation about symmetry axis	1055.88	983.53	66.34	31.53	983.53*
overtone - out-of-plane bend	2478.05	2043.37		378.43	2043.38*
overtone - H_3O^+ rotation	2111.76	1886.00		72.31	1886.00*
combination – out-of-plane bend + H_3O^+ rotation	2294.90	1915.78		1643.74	1915.78*

$3H{\cdot}D_2$

Vibration	ω (harm) (cm^{-1})	ν (anharm) (cm^{-1})	I (harm) (km mol^{-1})	I (anharm) (km mol^{-1})	Depert (cm^{-1})
in-phase IHB	2706.81	2351.99	1218.09	368.72	2347.09
out-of-phase IHB	2594.38	2248.91	3698.90	1125.78	2257.11
out-of-phase H_2O bend/H_3O^+ wag	1689.57	1633.80	57.82	3.07	1594.93
in-phase H_2O bend/H_3O^+ HOH bend	1684.97	1527.51	10.77	1.82	1544.97
in-phase H_2O bend/H_3O^+ HOH bend	1624.14	1621.34	1.60	1.23	1602.01
out-of-phase H_2O bend/H_3O^+ wag	1600.79	1544.50	9.97	18.36	1531.46
IHB out-of-plane bend (H_3O^+ umbrella)	1227.33	1071.04	207.30	108.33	1060.90
H_3O^+ rotation about symmetry axis	1053.17	986.10	67.55	35.35	986.10*
overtone - out-of-plane bend	2454.66	1986.64		253.49	1986.64*
overtone - H_3O^+ rotation	2106.34	1893.85		65.67	1893.85*
combination – out-of-plane bend + H_3O^+ rotation	2280.50	1900.73		1281.34	1900.73*

$3H{\cdot}N_2$

Vibration	ω (harm) (cm^{-1})	ν (anharm) (cm^{-1})	I (harm) (km mol^{-1})	I (anharm) (km mol^{-1})	Depert (cm^{-1})
in-phase IHB	2773.53	2450.59	1278.45	402.43	2452.57
out-of-phase IHB	2675.38	2337.27	3483.82	1338.65	2356.43
out-of-phase H_2O bend/H_3O^+ wag	1693.13	1636.32	43.48	2.94	1592.38
in-phase H_2O bend/H_3O^+ HOH bend	1685.11	1514.29	9.96	6.16	1529.12
in-phase H_2O bend/H_3O^+ HOH bend	1626.03	1622.97	1.04	5.92	1605.61
out-of-phase H_2O bend/H_3O^+ wag	1607.99	1579.51	22.63	1.69	1551.76
IHB out-of-plane bend (H_3O^+ umbrella)	1214.97	1067.33	215.55	76.55	1034.59
H_3O^+ rotation about symmetry axis	1034.58	961.02	68.93	35.85	958.33
overtone - out-of-plane bend	2429.94	1942.46		146.75	1942.46*
overtone - H_3O^+ rotation	2069.15	1844.03		53.97	1844.03*
combination – out-of-plane bend + H_3O^+ rotation	2249.54	1874.68		714.48	1874.68*

3H·CO

Vibration	ω (harm) (cm^{-1})	ν (anharm) (cm^{-1})	I (harm) (km mol^{-1})	I (anharm) (km mol^{-1})	Depert (cm^{-1})
in-phase IHB	2845.07	2610.27	1326.36	292.83	2603.62
out-of-phase IHB	2768.02	2523.75	3240.52	633.90	2520.76
out-of-phase H_2O bend/H_3O^+ wag	1695.21	1680.63	37.25	9.21	1584.39
in-phase H_2O bend/H_3O^+ HOH bend	1683.18	1497.29	7.84	6.29	1505.43
in-phase H_2O bend/H_3O^+ HOH bend	1628.52	1630.70	1.35	42.44	1626.81
out-of-phase H_2O bend/H_3O^+ wag	1614.04	1484.59	32.89	2.09	1563.86
IHB out-of-plane bend (H_3O^+ umbrella)	1193.98	963.53	213.63	97.61	987.15
H_3O^+ rotation about symmetry axis	1015.84	924.66	65.80	48.45	924.66*
overtone - out-of-plane bend	2387.96	1849.66		86.46	1849.66*
overtone - H_3O^+ rotation	2031.67	1784.15		42.30	1784.15*
combination – out-of-plane bend + H_3O^+ rotation	2209.82	1812.14		423.99	1812.14*

2H·MeOH

Vibration	ω (harm) (cm^{-1})	ν (anharm) (cm^{-1})	I (harm) (km mol^{-1})	I (anharm) (km mol^{-1})	Depert (cm^{-1})
in-phase IHB	2890.92	2571.23	1193.45	638.15	2568.05
out-of-phase IHB	2842.33	2384.57	3087.18	924.10	2471.39
in-phase H_2O bend/$MeOH_2^+$ HOH bend	1709.56	1648.17	0.20	0.33	1620.46
out-of-phase H_2O bend	1634.68	1578.98	38.17	13.37	1578.98*
in-phase H_2O bend/$MeOH_2^+$ HOH bend	1614.49	1556.42	55.02	12.82	1580.93
IHB out-of-plane bend (1) (H_3O^+ umbrella)	1222.95	1183.57	98.24	3.18	1117.67
IHB out-of-plane bend (2) (H_3O^+ umbrella)	1144.99	1038.10	58.25	126.72	1103.50
$MeOH_2^+$ HOH rotation about symmetry axis	982.65	898.29	74.95	45.33	898.29*
overtone - out-of-plane bend (1)	2445.90	2182.43		45.83	2182.43*
overtone - out-of-plane bend (2)	2289.97	2202.83		6.57	2199.60
overtone - $MeOH_2^+$ HOH rotation	1965.30	1732.70		34.21	1732.70*
combination - out-of-plane bend (1) + $MeOH_2^+$ HOH rotation	2205.60	1989.35		112.93	1989.35*
combination - out-of-plane bend (2) + $MeOH_2^+$ HOH rotation	2127.64	1989.00		35.84	1989.00*

2H·EtOH

Vibration	ω (harm) (cm^{-1})	ν (anharm) (cm^{-1})	I (harm) (km mol^{-1})	I (anharm) (km mol^{-1})	Depert (cm^{-1})
in-phase IHB	2936.81	2635.01	1317.63	988.76	2635.01*
out-of-phase IHB	2907.56	2577.69	2692.18	853.35	2578.71
in-phase H_2O bend/$EtOH_2^+$ HOH bend	1704.21	1647.55	3.14	1.62	1614.73
out-of-phase H_2O bend	1634.71	1583.98	41.72	25.33	1583.82
in-phase H_2O bend/$EtOH_2^+$ HOH bend	1616.63	1548.91	72.73	22.06	1579.48
IHB out-of-plane bend (1) (H_3O^+ umbrella)	1208.14	1145.52	106.45	1.65	1103.35
IHB out-of-plane bend (2) (H_3O^+ umbrella)	1131.93	1040.88	35.40	42.95	1084.69
$EtOH_2^+$ HOH rotation about symmetry axis	956.94	869.10	59.63	11.97	872.71
overtone - out-of-plane bend (1)	2416.27	2160.37		49.15	2160.37*
overtone - out-of-plane bend (2)	2263.86	2157.75		18.53	2157.75*
overtone - $EtOH_2^+$ HOH rotation	1913.87	1679.20		37.73	1679.20*
combination - out-of-plane bend (1) + $EtOH_2^+$ HOH rotation	2165.07	1946.32		78.84	1946.32*
combination - out-of-plane bend (2) + $EtOH_2^+$ HOH rotation	2088.87	1944.48		25.73	1944.48*

3D

Vibration	ω (harm) (cm^{-1})	ν (anharm) (cm^{-1})	I (harm) (km mol^{-1})	I (anharm) (km mol^{-1})	Depert (cm^{-1})
in-phase IDB	1894.29	1717.34	560.13	236.00	1670.53
out-of-phase IDB	1873.61	1696.91	1950.06	799.42	1608.73
out-of-phase D_2O bend/D_3O^+ wag	1226.05	1196.58	80.48	18.16	1192.59
in-phase D_2O bend/D_3O^+ DOD bend	1216.95	1147.55	3.79	2.95	1146.01
in-phase D_2O bend/D_3O^+ DOD bend	1189.45	1189.22	2.24	0.91	1174.47
out-of-phase D_2O bend/D_3O^+ wag	1152.66	1120.36	1.09	24.05	1112.34
IDB out-of-plane bend (D_3O^+ umbrella)	908.35	824.04	103.93	80.61	824.04*
D_3O^+ rotation about symmetry axis	772.86	735.60	23.72	1.78	735.60*
overtone - out-of-plane bend	1816.70	1558.40	118.55	164.33	1609.61
overtone - D_3O^+ rotation	1545.72	1429.34	28.35	86.83	1429.34*
combination – out-of-plane bend + D_3O^+ rotation	1681.21	1455.49	475.57	819.66	1543.67

3D·D_2

Vibration	ω (harm) (cm^{-1})	ν (anharm) (cm^{-1})	I (harm) (km mol^{-1})	I (anharm) (km mol^{-1})	Depert (cm^{-1})
in-phase IDB	1950.08	1754.73	573.31	305.17	1731.92
out-of-phase IDB	1941.58	1733.01	1821.43	1014.00	1739.35
out-of-phase D_2O bend/D_3O^+ wag	1226.45	1220.23	77.80	11.41	1183.43
in-phase D_2O bend/D_3O^+ DOD bend	1217.29	1137.45	2.59	0.79	1143.58
in-phase D_2O bend/D_3O^+ DOD bend	1191.54	1190.70	1.18	0.04	1175.19
out-of-phase D_2O bend/D_3O^+ wag	1161.97	1118.47	0.02	12.66	1122.56
IDB out-of-plane bend (D_3O^+ umbrella)	893.56	796.18	100.61	52.71	793.51
D_3O^+ rotation about symmetry axis	758.68	724.37	22.93	13.26	724.37*
overtone - out-of-plane bend	1787.12	1516.85		46.38	1545.51
overtone - D_3O^+ rotation	1517.36	1410.16		21.04	1410.16*
combination – out-of-plane bend + D_3O^+ rotation	1652.24	1451.06		294.04	1451.06*

$3D{\cdot}N_2$

Vibration	ω (harm) (cm^{-1})	ν (anharm) (cm^{-1})	I (harm) (km mol^{-1})	I (anharm) (km mol^{-1})	Depert (cm^{-1})
in-phase IDB	1998.48	1838.94	584.58	293.82	1842.89
out-of-phase IDB	1997.50	1799.75	1722.53	564.99	1799.75*
out-of-phase D_2O bend/D_3O^+ wag	1227.35	1202.35	68.48	24.78	1182.49
in-phase D_2O bend/D_3O^+ DOD bend	1216.53	1124.39	2.17	0.23	1136.37
in-phase D_2O bend/D_3O^+ DOD bend	1193.14	1201.60	1.66	1.51	1184.56
out-of-phase D_2O bend/D_3O^+ wag	1169.74	1161.42	2.22	3.83	1136.93
IDB out-of-plane bend (D_3O^+ umbrella)	885.59	811.55	104.69	24.29	785.50
D_3O^+ rotation about symmetry axis	745.20	703.65	24.27	15.89	703.25
overtone - out-of-plane bend	1771.19	1497.53	63.88	146.75	1497.53*
overtone - D_3O^+ rotation	1490.39	1370.78	16.84	53.97	1370.78*
combination – out-of-plane bend + D_3O^+ rotation	1630.79	1436.97	189.19	714.48	1436.97*

3D·CO

Vibration	ω (harm) (cm^{-1})	ν (anharm) (cm^{-1})	I (harm) (km mol^{-1})	I (anharm) (km mol^{-1})	Depert (cm^{-1})
in-phase IDB	2062.03	1932.78	1605.62	327.96	1171.88
out-of-phase IDB	2049.99	1926.67	551.05	284.64	1926.67*
out-of-phase D_2O bend/D_3O^+ wag	1227.70	1237.90	63.24	8.17	1171.88
in-phase D_2O bend/D_3O^+ DOD bend	1214.05	1097.12	1.70	0.51	1111.61
in-phase D_2O bend/D_3O^+ DOD bend	1195.12	1221.83	2.77	18.43	1206.95
out-of-phase D_2O bend/D_3O^+ wag	1176.46	1074.05	5.50	5.39	1156.57
IDB out-of-plane bend (D_3O^+ umbrella)	871.26	739.53	103.51	49.63	759.46
D_3O^+ rotation about symmetry axis	731.49	683.92	23.89	18.79	683.92*
overtone - out-of-plane bend	1742.53	1447.01		35.13	1447.01*
overtone - D_3O^+ rotation	1462.97	1335.63		13.01	1335.63*
combination – out-of-plane bend + D_3O^+ rotation	1602.75	1397.83		123.76	1397.83*

*Denotes situations where due to the absence of nearly degenerate states, no deperturbation analysis was performed. As a result, the deperturbed frequencies are the same as the anharmonic frequencies.

Table S7. Band labels, experimental frequencies, and assignments for **3D$_6$H**·D$_2$ and its three isotopologues with the proton in the free OH of the flanking waters (**3D$_6$H$_{free}$**), free OH of the hydronium core bound to a tag (**3D$_6$H$_{tag\ \text{bound}}$**), and in the shared proton of the hydronium core bound to a flanking water (**3D$_6$H$_{bound}$**), relevant to Fig. 5 and Fig. S4.

Label 3D·D$_2$	**Label 3D$_6$H·D$_2$ (VSCF/VCI)**	**[a]Exp. 3D$_6$H·D$_2$**	**[a]Exp. 3D$_6$H$_{free}$·D$_2$**	**VSCF/VCI 3D$_6$H$_{free}$**	**[a]Exp. 3D$_6$H$_{tb}$·D$_2$** *tb = tag bound*	**VSCF/VCI 3D$_6$H$_{tb}$** *tb = tag bound*	**[a]Exp. 3D$_6$H$_{bound}$·D$_2$**	**VSCF/VCI 3D$_6$H$_{bound}$**	**Assignments based on VSCF/VCI calculations**
	c_1 (γ_1)	3685	3685	3681			3685	-	Free OH HDO stretch
	c_2 (γ_2)	3575			3575	3630			Free OH HD_2O^+ stretch
	c_3 (γ_3)	3491[b]							
ν^{D_2}		2960							D_2 stretch[c]
*	*	2831	2831		2831				D_2O antisym. stretch + D_3O^+ torsion[3]
b_1	c_4 (γ_4)	2771	2771	2778	2771	2783	2771	2779	Free OD antisym. D_2O stretch
	c_5 (γ_5)	2704	2704	2715					Free OD HDO stretch
b_2	c_6 (γ_6)	2653	2653	2659	2653	2662	2653	2663	Free OD sym. D_2O stretch
b_3	c_7 (γ_7)	2629	2629	2688			2629	2693	Free OD D_3O^+/HD_2O^+ stretch
b_4	c_8 (γ_8)	2356							Combination band of D_3O^+ bend + water bend
	c_9 (γ_9)	2284[b]							
b_5	c_{10} (γ_{10})	2164							Mixed states involving the IDB
b_6	c_{11a} (γ_{11a})	2059			2059	2084	2059	2120	Mixed states involving the IHB
	c_{11b} (γ_{11b})	1978	1978	1996					Mixed states involving the IDB
b_7	c_{12} (γ_{12})	1807			1807	1836	1830	1919	Mixed states involving the IHB + IDB
b_{8a}	c_{13} (γ_{13})	1774	1774	1851			1793	1880	Mixed states involving the IHB + IDB
b_{8b}	c_{14} (γ_{14})	1672	1672	1740	1672	1715	1687	1706	Mixed states involving the IDB
	c_{15} (γ_{15})	1477	1477	1533	1477	1573			Mixed states involving the IDB
	c_{16} (γ_{16})	1423	1423	1482			1423	1460	Mixed states involving the IDB
	c_{17} (γ_{17})	1354			1354	1371			Mixed states involving the IDB
b_9	c_{18} (γ_{18})	1207	1207	1215					D_3O^+ bend
b_{10}	c_{19} (γ_{19})	1144							D_2O bend

[a]Experimental frequencies are accurate within ±4 cm^{-1}.

[b]Unassigned features.

[c]Assigned based on proximity to D_2 stretch fundamental at 2993.6 cm^{-1} and not VSCF/VCI calculations.[5]

Table S8. The matrix elements (cm^{-1}) for the F-G analysis of the coupling between the out-of-phase shared proton stretch and the two bending modes determined based on a transition state structure in which the hydronium core and the three oxygen atoms lie in a plane, while the water molecules lie in planes that are perpendicular to the plane containing the oxygen atoms. The H_2 molecule also lies perpendicular to the plane of the oxygen atoms, while CO and N_2 are collinear to the free OH bond in the **3H** core. The analysis is performed using both the local harmonic OH stretch frequency (harm IHB) and an approximation to the anharmonic local frequency (anharm IHB), obtained by scaling the frequency by the ratio of the VPT2 to the harmonic frequency of this vibration obtained at the same level of theory. In both cases, the bend frequency is harmonic. In this analysis, the two bends are decoupled from each other and each bend is allowed to couple to the IHB OH stretch at the harmonic level through both potential (F) and kinetic (G) coupling terms. The first row indicates values for **3H**, while the rows associated with the tags (X=H_2, N_2, CO) indicate changes from those bare values. Bend 1 and bend 2 have mixed character comprised of the exterior H_2O bend and H_3O^+ wag in the **3H** system and the blue shifts seen in the Bend 1 and Bend 2 columns for diagonal elements reflects an increase in frequency of the free OH wagging vibration in H_3O^+ with increased tag strength.

The Matrix Elements (cm^{-1}) for the F-G Analysis

System	Bend 1 (cm^{-1})	Bend 2 (cm^{-1})	Harm IHB (cm^{-1})	Anharm IHB (cm^{-1})	IHB-bend 1 (F) (cm^{-1})	IHB-bend 1 (G) (cm^{-1})	IHB-bend 2 (F) (cm^{-1})	IHB-bend 2 (G) (cm^{-1})
	Diagonal Elements				Off Diagonal Elements			
3H	1652.32	1614.21	2451.24	1855.28	-135.57	86.67	329.87	133.57
	Shifts from **3H**				Shifts from **3H**			
3H·H_2	10.31	11.00	113.19	363.11	-90.26	40.83	-3.99	-23.59
3H·N_2	17.50	14.9	202.79	463.61	-127.99	59.57	-20.89	-38.57
3H·CO	26.29	17.19	301.71	654.29	-118.89	76.02	-44.13	-52.82

Table S9. Frequencies obtained by performing a F-G analysis using the matrix elements provided in Table S8. The first three columns are the frequencies obtained when the shared proton stretch is treated as a harmonic oscillator, and the second set of frequencies use the anharmonic frequency for the shared proton stretch. The first row indicates values for **3H**, while the rows associated with the tags (X=H_2, N_2, CO) indicate changes from those bare values. Bend 1 and bend 2 have mixed character comprised of the exterior H_2O bend and H_3O^+ wag in the **3H**.

Fundamental Frequencies Obtained by Performing an F-G Analysis Using the Matrix Elements Provided in Table S8

	Harmonic IHB			Anharmonic IHB		
System	**Bend 1 (cm^{-1})**	**Bend 2 (cm^{-1})**	**IHB (cm^{-1})**	**Bend 1 (cm^{-1})**	**Bend 2 (cm^{-1})**	**IHB (cm^{-1})**
3H	1550.75	1649.46	2506.70	1467.91	1649.03	1992.10
			Shifts from **3H**			
3H·H_2	22.84	10.19	103.18	81.40	10.17	295.63
3H·N_2	35.21	15.98	186.32	100.11	15.64	383.78
3H·CO	46.87	22.95	279.01	120.98	22.53	559.36

The comparison of the results in Tables S8 and S9 show that the fundamentals of the higher frequency bend normal mode (bend 2) follow the same pattern was seen for the uncoupled bends (see Table S8). The frequency of the bend 1 normal mode shows greater tag dependence, and this is more pronounced when anharmonic frequencies are used for the IHB. This serves to illustrate the fact that with the blue-shift of the shared proton stretch, the mixing with the bends decreases, accounting for the observed blue shifts of this band with increasing interaction with the tag. A second, contributor to the shifts is seen in an underlying blue-shift of the bend frequencies (see the bend 1 and bend 2 columns in Table S8) with increased tag strength. Depending on the frequency of the IHB, this factor is typically smaller than the shift that comes from the reduction in mixing of these vibrations in the construction of the normal modes.

Methods 1: VPT2 approaches and discussion of findings

As we consider the frequencies that are obtained from the VPT2 calculations, it is useful to start by remembering that such calculations have their limitations with respect to assignments when considering strongly coupled and anharmonic ions, like **3H** or **3D**. In the present study a degenerate form of VPT2 is employed. For these calculations, the Hamiltonian is partitioned into those terms that couple nearly degenerate states, H_{deg}, and those that do not, $H_{non\text{-}deg}$, and the Hamiltonian is replaced by $H_{non\text{-}deg}$ for the purposes of calculating the second-order corrected, deperturbed energies. These deperturbed energies then become the diagonal elements for a reduced Hamiltonian that only includes the nearly degenerate states and the couplings between them. As noted in the text and in the results in Table S6, there are several excited states, which have excitation in vibrations that correspond to hindered rotations or the umbrella motion of the hydronium core, that are close in energy to the first excited state of the H-bonded OH stretch. While the results of VPT2 calculations performed using G16, reported in Table S6, indicate an assignment of a transition to excitations in one or two of the normal modes, in fact these excited states are linear combinations of several zero-order vibrationally excited levels, and the assignments reported in that table represent the leading contribution, which in some cases is lower than 50%. On the other hand, we can use the energies calculated using VPT2 to explore trends in the frequencies of specific vibrationally excited states of **3H** or **3D** upon the introduction of a tag molecule or through substitution of the free OH with a methyl or ethyl group. We also find (see Figure S5) that the spectra calculated using VPT2 provide a good qualitative description of the general spectral features.

For example, as the interaction strength of the tag with the **3H** or **3D** is increased, the calculated harmonic or anharmonic frequencies of the IHB or IDB also increase. This pulls these excited states out of resonance with the excited states that are assigned as overtones and combination bands in Table S6. At the same time, the intensities of these two quanta transitions decrease with increasing tag strength. This loss of intensity in the two quanta transitions with increased tag strength indicates that these transitions are borrowing intensity from the bright H-bonded OH stretch vibration in **3H** where the excited states are close in energy. As the frequency of the H-bonded OH stretch shifts to higher energy, it moves out of resonance with these excited states, and their intensity drops, while the frequency of the transition remains roughly constant.

Based on the VPT2 calculations, the frequencies of the overtone and combination states reported in Table S6 shift by less than 100 cm^{-1} when we consider the D_2, N_2 and CO tags on **3H**. This shift is much smaller than the corresponding shift in the IHB frequencies, which are more than 300 cm^{-1}. While the magnitudes of the shifts are smaller in **3D** compared to **3H**, the relative shifts of the fundamental in the IDB compared to the combination bands follow the same trends as are described for **3H**. When the free OH in **3H** is replaced by a methyl or ethyl group, blue-shifts in the H-bonded OH stretches are found in both the measured spectrum and VPT2 results.

While not providing definitive assignments, the results of the VPT2 calculations support the experimental approach, taken in this study, in which we take advantage of the sensitivity of the frequency response of the H-bonded OH stretch vibrations to the environment. In doing so, we gather the frequency of the underlying OH stretch vibration by extrapolating the trends obtained as the interaction between the hydronium free OH with the tag is increased.

Methods 2: DMC approaches for calculating band origin for H-bonded OH stretch

The anharmonic frequency of the H-bonded OH stretches in **3H** obtained from DMC is based on the DMC calculation described elsewhere.[9] The ensembles of walkers that were used to provide the probability amplitude in that study were first symmetrized by permuting the two equivalent H…OH_2 units, the two hydrogen atoms in the dangling waters and performing a reflection of the ion in the plane that contains the three O atoms. In this way, each walker is replaced by 16 energetically equivalent structures. The excited state energy is calculated based on this wave function using the approaches described in ref. 10-11. In that approach, we approximate the excited state in the H-bonded OH stretch of the hydronium core by

$$|\Psi_1\rangle \approx (q - \langle q \rangle)|\Psi_0\rangle \quad \text{(S1)}$$

where q represents a linear combination of the internal displacement coordinates. The coefficients for this transformation are the eigenvectors of the matrix of second moments of the ground state probability amplitude evaluated in mass-weighted internal coordinates diagonalizing the matrix of second moments, $\mathbf{M}^{(MW)}$ in internal coordinates,

$$\mathbf{M}^{MW} = \mathbf{G}^{-\frac{1}{2}}\mathbf{M}\mathbf{G}^{-\frac{1}{2}} \quad \text{(S2)}$$

where **G** is the Wilson G-matrix[12] and

$$\boldsymbol{M_{ij}} = \langle (\boldsymbol{r_i} - \langle \boldsymbol{r_i} \rangle)\left(\boldsymbol{r_j} - \langle \boldsymbol{r_j} \rangle\right)\rangle \quad \text{(S3)}$$

For this calculation, the twenty four internal coordinates that define the geometry of **3H** consist of: Seven OH bond lengths; Three HOH angles, one for each of the two water molecules and the angle involving the two H-bonded OH bonds in the hydronium core; Two OO distances between the oxygen atoms in each of the water molecules and the hydronium ion; The associated OOO angle; The orientation of the free OH bond in the hydronium core, which is defined using two spherical coordinates; Three Euler angles for each water molecule; Three Euler angles for the hydronium core. The Euler angles are based on a reference structure in which the hydronium ion is planar, and the water molecules are oriented to be perpendicular to the plane that contains the three oxygen atoms.

In this calculation, we focus on the collective coordinate, q, that most closely resembles the out-of-phase displacements of the two H-bonded OH stretching vibrations along the O-O bonds. Within this formalism,

$$\nu = \langle \mathrm{T} \rangle_1 - \langle \mathrm{T} \rangle_0 + \langle \mathrm{V} \rangle_1 - \langle \mathrm{V} \rangle_0 \quad \text{(S4)}$$

where

$$\langle T\rangle_1 - \langle T\rangle_0 = \frac{n\hbar^2\alpha}{2m} \quad \text{(S5)}$$

$$\alpha = \frac{\langle q^2\rangle}{\langle q^4\rangle - \langle q^2\rangle^2} \quad \text{(S6)}$$

and

$$\langle V\rangle_1 - \langle V\rangle_0 = \langle (q - \langle q\rangle)V(q - \langle q\rangle)\rangle_0 - \langle V\rangle_0 \quad \text{(S7)}$$

In the above expressions, the 0 and 1 subscripts represent averages over the ground or first excited state in *q*. Earlier studies on $H_3O_2^-$ from ref. 10 and **2H** from ref. 11 showed that it provides an accurate representation of the frequency of the fundamentals in similar ions.

References:

(1) Duong, C. H.; Gorlova, O.; Yang, N.; Kelleher, P. J.; Johnson, M. A.; McCoy, A. B.; Yu, Q.; Bowman, J. M. Disentangling the Complex Vibrational Spectrum of the Protonated Water Trimer, $H^+(H_2O)_3$, with Two-Color IR-IR Photodissociation of the Bare Ion and Anharmonic VSCF/VCI Theory. *J. Phys. Chem. Lett.* **2017,** *8*, 3782-3789.

(2) Hunter, E. P.; Lias, S. G. Proton Affinity Evaluation. In *NIST Chemistry WebBook, NIST Standard Reference Database Number 69*, Linstrom, P. J.; Mallard, W. G., Eds. National Institute of Standards and Technology: Gaithersburg MD, 20899, 2019.

(3) Douberly, G. E.; Walters, R. S.; Cui, J.; Jordan, K. D.; Duncan, M. A. Infrared Spectroscopy of Small Protonated Water Clusters, $H^+(H_2O)_n$ (n=2-5): Isomers, Argon Tagging, and Deuteration. *J. Phys. Chem. A* **2010,** *114*, 4570-4579.

(4) Wolke, C. T.; Fournier, J. A.; Dzugan, L. C.; Fagiani, M. R.; Odbadrakh, T. T.; Knorke, H.; Jordan, K. D.; McCoy, A. B.; Asmis, K. R.; Johnson, M. A. Spectroscopic Snapshots of the Proton-Transfer Mechanism in Water. *Science* **2016,** *354*, 1131-1135.

(5) Dickenson, G. D.; Niu, M. L.; Salumbides, E. J.; Komasa, J.; Eikema, K. S. E.; Pachucki, K.; Ubachs, W. Fundamental Vibration of Molecular Hydrogen. *Phys. Rev. Lett.* **2013,** *110*, 193601.

(6) Coblentz Society, I. Evaluated Infrared Reference Spectra. In *NIST Chemistry WebBook, NIST Standard Reference Database Number 69*, Linstrom, P. J.; Mallard, W. G., Eds. National Institute of Standards and Technology: Gaithersburg MD, 20899, 2019.

(7) Lofthus, A.; Krupenie, P. H. Spectrum of Molecular Nitrogen. *J. Phys. Chem. Ref. Data* **1977,** *6*, 113-307.

(8) Frisch, M. J.; Trucks, G. W.; Schlegel, H. B.; Scuseria, G. E.; Robb, M. A.; Cheeseman, J. R.; Scalmani, G.; Barone, V.; Petersson, G. A.; Nakatsuji, H., et al. *Gaussian 16 Rev. A.03*, Wallingford, CT, 2016.

(9) Dzugan, L. C.; DiRisio, R. J.; Madison, L. R.; McCoy, A. B. Spectral Signatures of Proton Delocalization in $H^+(H_2O)_{n=1-4}$ Ions. *Faraday Discuss.* **2018,** *212*, 443-466.

(10) McCoy, A. B.; Diken, E. G.; Johnson, M. A. Generating Spectra from Ground-State Wave Functions: Unraveling Anharmonic Effects in the $OH^-{\cdot}H_2O$ Vibrational Predissociation Spectrum. *J. Phys. Chem. A* **2009,** *113*, 7346-7352.

(11) Guasco, T. L.; Johnson, M. A.; McCoy, A. B. Unraveling Anharmonic Effects in the Vibrational Predissociation Spectra of $H_5O_2^+$ and Its Deuterated Analogues. *J. Phys. Chem. A* **2011,** *115*, 5847-5858.

(12) Wilson, E. B.; Decius, J. C.; Cross, P. C. *Molecular Vibrations: The Theory of Infrared and Raman Vibrational Spectra*. McGraw Hill: New York, 1955.